Structural rearrangements and selection promote phenotypic evolution in *Anolis* lizards

Raúl Araya-Donoso[1], Sarah M. Baty[1], Jaime E. Johnson[1], Eris Lasku[1], Jody M. Taft[2], Rebecca E. Fisher[1], Jonathan Losos[3], Greer A. Dolby[4], Kenro Kusumi[1], Anthony J. Geneva[2*]

1: School of Life Sciences, Arizona State University, Tempe, AZ 85287 USA

2: Department of Biology & Center for Computational and Integrative Biology, Rutgers University–Camden, Camden, NJ 08103 USA

3: Department of Biology, Washington University, Saint Louis, MO, USA

4: Department of Biology, University of Alabama at Birmingham, AB, USA

***:** Correspondence to anthony.geneva@rutgers.edu

Short title: Structural variation and selection in *Anolis*

Abstract

The genomic characteristics of adaptively radiated groups could contribute to their high species number and ecological disparity, by increasing their evolutionary potential. Here, we explored the genomic variation of *Anolis* lizards, focusing on three species with distinct phenotypes: *A. auratus*, one of the species with the longest tail; *A. frenatus*, one of the largest species; and *A. carolinensis*, one of the species that inhabits the coldest environments. We assembled and annotated two new chromosome-level reference genomes for *A. auratus* and *A. frenatus*, and compared them with the available genomes of *A. carolinensis* and *A. sagrei*. We evaluated the presence of structural rearrangements, quantified the density of repeat elements, and identified potential signatures of positive selection in coding and regulatory regions. We detected substantial rearrangements in scaffolds 1, 2 and 3 of *A. frenatus* different from the other species, in which the rearrangement breakpoints corresponded to hotspots of developmental genes. Further, we detected an accumulation of repeats around key developmental genes in anoles and phrynosomatid outgroups. Finally, coding sequences and regulatory regions of genes relevant to development and physiology showed variation that could be associated with the unique phenotypes of the analyzed species. Our results show examples of the hierarchical genomic variation within anoles, that could provide the substrate that promoted phenotypic disparity and contributed to their adaptive radiation.

Key words: adaptive radiation, comparative genomics, reference genome, transposable elements.

Significance

In this study, we generated high-quality reference genome assemblies and annotations for two species of anole lizards. Our analyses show examples of some genomic characteristics within the *Anolis* adaptive radiation that could be associated with the high diversity found in the genus. These genomes are valuable resources for comparative genomics and evolutionary biology research, as they can aid future research efforts to link the genomic variation of organisms with their evolutionary potential.

Introduction

Adaptively radiated groups of organisms are natural experiments in which the relative roles of ecological and genomic factors on speciation and phenotypic differentiation can be assessed (Gillespie et al. 2020; Martin & Richards 2019; Schluter 2000). In general, ecological variation and the emergence of ecological opportunity are known to play an important role in determining the ability of a group of organisms to radiate adaptively (Stroud & Losos 2016; Wellborn & Langerhans 2015). On the other hand, genetic mechanisms could also influence the ability of organisms within radiations to diversify and generate extensive phenotypic variation because clades with greater evolutionary potential could be more likely to radiate adaptively (Gillespie et al. 2020; Seehausen et al. 2014). Multiple genetic mechanisms could contribute to increased genetic and phenotypic diversity such as chromosome-level structural rearrangements, small-scale structural variation, the dynamics of transposable elements, mutation rates, recombination rates, and the genomic landscape of selection on regulatory elements and/or coding regions (Bourque et al. 2018; Brawand et al. 2014; Han et al. 2017; Mérot et al. 2020; Seehausen et al. 2014).

The relevance of the genomic substrate for highly speciose or adaptively radiated groups of organisms has been discussed before. For example, African lake cichlids show ancient genetic polymorphisms, structural rearrangements, high divergence in regulatory sequences, insertion of transposable elements within regulatory elements, and novel miRNAs (Brawand et al. 2014; McGee et al. 2020; Seehausen et al. 2014). Darwin's finches also exhibit evidence of ancient polymorphisms, and selection on large-effect loci associated with beak morphology located in genomic islands of low recombination (Han et al. 2017; Rubin et al. 2022). *Heliconius* butterflies present increased genomic variation by

hybridization and/or introgression processes, high variability in regulatory regions, genome expansion events caused by an increase in repeat elements, and structural rearrangements (Edelman et al. 2019; Kozak et al. 2021; Lewis & Reed 2019; Seixas et al. 2021). Therefore, groups that radiate could have more labile genomes that allow for greater phenotypic diversification. A current challenge is to determine the relative importance of each of these genomic factors, and whether different radiations present similar genomic variation that aided diversification, or whether different radiations have occurred through different genomic mechanisms.

Anolis lizards are an ideal group to assess the relevance of genetic mechanisms for generating and promoting phenotypic diversity. This genus is described as an adaptive radiation with ~400 species distributed in the tropical Americas (Losos 2011; Muñoz et al. 2023). *Anolis* are considered a model system for evolutionary biology studies because they present extensive phenotypic variation across multiple niche axes. A remarkable characteristic of *Anolis* evolution is the repeated occurrence of intra-island radiation and morphological differentiation associated with microhabitat use patterns (Huie et al. 2021; Losos 1990; Mahler et al. 2010). Besides morphology, anoles have diversified in behavior, physiology, and sexual dimorphism (Butler et al. 2007; Gunderson et al. 2018; Velasco et al. 2016). In this context, anoles present a wide range of phenotypic variation compared to other taxa, and this diversity may be promoted by ecological and genetic mechanisms.

Within the *Anolis* radiation, some species have disparate phenotypes that could be adaptive to their niches (Fig. 1A). We focused on body size, tail length, and cold tolerance as ecologically meaningful traits with high variation within *Anolis* (Mahler et al. 2010, Table S1), and particularly variable among the *Anolis* species with genome assemblies

available. For example, *A. frenatus* is among the larger anole species (Fig. 1B), which may reduce its predation risk and enable a wider dietary breadth, potentially including other anole lizards as prey (Losos et al. 1991); *A. auratus* inhabits grasslands and perches on narrow branches and features an extremely long tail (Fig. 1C), a trait that may provide better balance in species that walk and jump along narrow surfaces (Gillis et al. 2009; Hsieh 2015); and *A. carolinensis* is one of the species with highest cold tolerance (Fig. 1D), enabling its colonization towards higher latitudes and survival during cold seasons (Campbell-Staton et al. 2018). Different types of genomic variation, particularly within coding regions, may control such traits. For instance, longer tails could be produced by modifications of the number and/or size of the caudal vertebrae, controlled by molecular pathways involved in the axial skeleton development (Bergmann & Morinaga 2019; Mallo 2018, 2020). A larger body size could be controlled by insulin growth factor or growth hormone pathways (Beatty & Schwartz 2020; Duncan et al. 2020; Rotwein 2018), while cold adaptation could be related to genes regulating oxygen consumption and/or blood circulation (Campbell-Staton et al. 2018; Pörtner H. 2001).

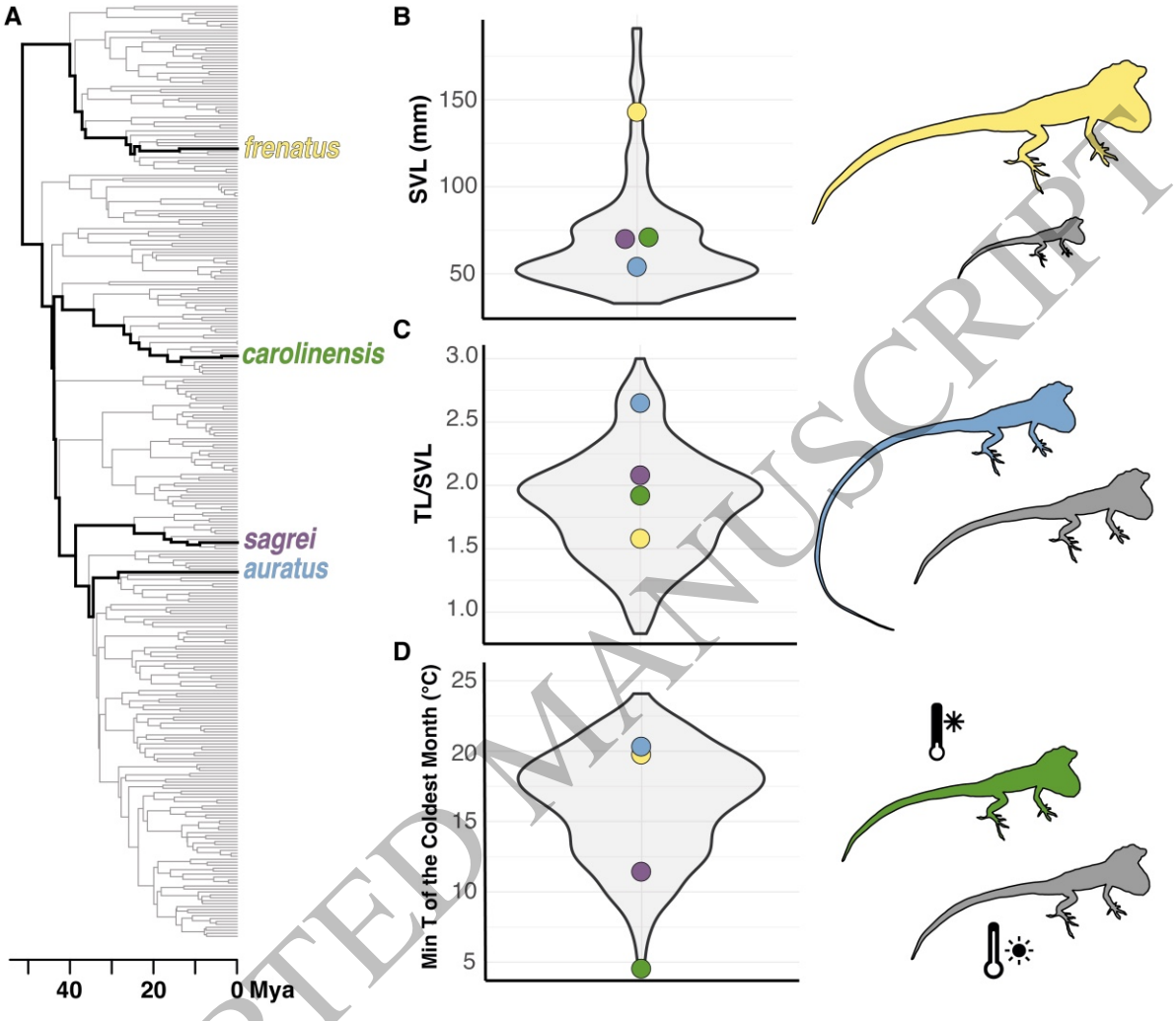

Figure 1. *Anolis* phylogenetic relationships (**A**) and genus-wide phenotypic variation in snout-vent length (SVL; **B**), tail length (TL; **C**), and thermal climatic niche (**D**), highlighting the species included in this study (Phylogenetic and morphological data from Poe et al., (2017); temperature data obtained from WorldClim 2 (Fick & Hijmans 2017) for all species).

A variety of genomic characteristics have been hypothesized to play a role in the great ecological disparity observed among *Anolis* species. Tollis et al. (2018) compared short-read genome assemblies of five species (including *A. carolinensis*, *A. auratus* and *A. frenatus*), and detected high mutation rates in anoles compared to other vertebrates, and signatures of natural selection on genes associated with limb and brain development and hormonal regulation. In some Cuban anole species, an accumulation of gene duplications has been reported (Kanamori et al. 2022), and genomic regions undergoing accelerated evolution have been identified in association with thermal biology (Sakamoto et al. 2024). Furthermore, *Anolis* genetic diversity could have been fueled by ancient hybridization and introgression processes (Farleigh et al. 2023; Wogan et al. 2023). Chromosomal rearrangements could also be relevant because multiple events of chromosome gains and losses have been described within *Anolis* (Castiglia et al. 2013; Gamble et al. 2014), and chromosome fission and fusions have been proposed to determine the evolution of the *Anolis* X chromosome (Geneva et al. 2022; Giovannotti et al. 2017). Finally, the dynamics of repeat elements could be relevant because transposable elements can impact the genome by modifying gene regulation patterns, causing mutations, or promoting genome rearrangements (Bourque et al. 2018). A high density of transposable elements within the *hoxB and hoxC* gene clusters, key regulators of morphological development, has been reported in *Anolis* (Feiner 2016, 2019; Di-Poï et al. 2010). Nonetheless, genome-wide patterns associated with repeat density and structural rearrangements remain to be explored with chromosome-level genome assemblies.

Here, we explored the genomic variation of species with disparate phenotypes within the adaptively radiated *Anolis* group. We generated chromosome-level reference

genomes for two *Anolis* species and found evidence for major structural rearrangements, described a unique pattern of repeat density through the genome, and identified genes putatively under positive selection. We hypothesize that this variation could influence the unique traits of four species representing divergent phenotypes. By analyzing a subset of the anole radiation these results show an example of the potentially diverse genomic architecture within *Anolis*, which could fuel genetic diversity and hence, promote the high diversification and phenotypic disparity in the genus.

Results

Chromosome level genome assemblies and annotation for A. auratus *and* A. frenatus

We generated chromosome-level genome assemblies for two *Anolis* species (Table 1). Both type specimens were adult females from Panama (Table S2). The total sequencing coverage was 259x (116x short reads, 70x Chicago, and 73x Hi-C) for *A. auratus* and 370x (105x short reads, 128x Chicago, and 137x Hi-C) for *A. frenatus*. The resulting assemblies were contiguous (*A. auratus*: 281.8 Mbp of N50 and 0,916% gap; *A. frenatus* 342.7 Mbp of N50 and 1,464% gap) and moderately complete (BUSCO eukaryotic completeness of 93.07% for *A. auratus* and 86.14 % for *A. frenatus*). The percentage of missing genes could be attributed to highly fragmented contigs in the assemblies (Contig N50: *A. auratus* 18.64 Kbp; *A. frenatus* 10.19 Kbp). Both species show a similar pattern of repetitive element composition (Fig. S1), which corresponds to roughly 50% of the genome. However, *A. auratus* shows a recent accumulation of LINEs. We generated genome annotations for both species via the MAKER pipeline (Campbell et al. 2014) using a combination of new data,

and the proteomes of previously sequenced species (see Methods for details). For *A. auratus* we identified 19,879 genes with an average length of 19,877 bp (Table 1, Table S3), and 88.2% of all eukaryote BUSCO genes present in the annotation (either complete or fragmented), whereas for *A. frenatus* 19,643 genes were identified with an average length of 18,033 bp (Table 1, Table S3) and 76.1% eukaryotic BUSCO genes present. For subsequent analyses, our newly annotated genomes were compared against the chromosome-level reference genomes of *A. carolinensis* (AnoCar2.0, Alföldi et al. 2011; and DNAzoo Hi-C Assembly, Dudchenko et al. 2017, 2018) and *A. sagrei* (AnoSag2.1, Geneva et al. 2022), along with the phrynosomatid lizards *Urosaurus nigricaudus* (Davalos-Dehullu et al. 2023) and *Phrynosoma platyrhinos* (Koochekian et al. 2022).

Table 1. Genome assembly and annotation statistics for the four analyzed *Anolis* species.

Species	***A. auratus***	***A. frenatus***	***A. carolinensis***	***A. sagrei***
Genome version	RUC_Aaur_2	RUC_Afre_2	AnoCar2.0	AnoSag2.1
Assembly length (Gbp)	1.77	1.85	1.79	1.66
N50 (Mbp)	281.8	342.7	150.6	253.6
L50 (n°)	3	3	5	4
Eukaryote BUSCO Assembly (%)	C + F: 93.07	C + F: 86.14	C + F: 94.5%	C + F: 100%
% Repeats	48.53	51.27	33	46.3
N° genes	19,879	19,643	21,555	20,033
Average gene length (bp)	19,877	18,033	32,969	45,059
Eukaryote BUSCO Annotation (%)	C + F: 88.2	C + F: 76.1	C + F: 94.5%	C + F: 99.7%
Reference	This study	This study	Alföldi et al. 2011	Geneva et al. 2022

Chromosome-level structural rearrangements

We performed *in silico* chromosome painting to assess the synteny conservation among our four *Anolis* species and *U. nigricaudus* and *P. platyrhinos*, using *A. sagrei* as a reference. Overall, there is high synteny conservation for the main scaffolds or macrochromosomes among those species (Fig. 2A). Interestingly, scaffolds 1, 2, and 3 contain substantial structural rearrangements that are unique to *A. frenatus* (Fig. 2A, Fig. 2B). The Hi-C data for *A. frenatus* shows higher contact density within scaffolds and very little interaction between scaffolds 1, 2 and 3 (Fig. 2C, Fig. S2). This observation suggests that the observed rearrangements are not a sequencing or scaffolding artifact, but rather supports genuine structural differences in this species relative to other Iguanian taxa.

Structural rearrangements can modify the gene regulation and affect recombination patterns (Damas et al. 2021; Mérot et al. 2020). Therefore, we identified the genes located within 1 Mbp to the rearrangement breakpoints in scaffolds 1, 2 and 3 between *A. sagrei* and *A. frenatus* (Table S4) to hipothesize functional implications of this mutation. We conducted an enrichment analysis on the list of genes co-located to the breakpoints with g:Profiler (Kolberg et al. 2023) which showed significant enrichment of biological processes such as "cellular differentiation", "developmental process" and "pigment granule transport" (Table S5). Further, we quantified the density of genes associated with developmental GO terms along scaffolds 1, 2 and 3 of *A. frenatus*, and we detected that the chromosomal breaks were located in hotspots of genes with developmental functions (Fig. 2D). Among the genes contiguous to the rearrangement breakpoints (Table S4) we identified *axin2*, a regulator of the Wnt/β-catenin and TGF-β pathways that determines chondrocyte maturation and axial skeletal development (Dao et al. 2010); *bmp2*, a growth factor determinant for bone development through the BMP-Smad pathway (Shu et al.

2011); *ddit3*, transcription factor that influences myogenesis by regulating the GH-IGF1 pathway (Zecchini et al. 2019); and *twist2*, a transcription factor relevant for bone formation and myogenesis (Liu et al. 2017).

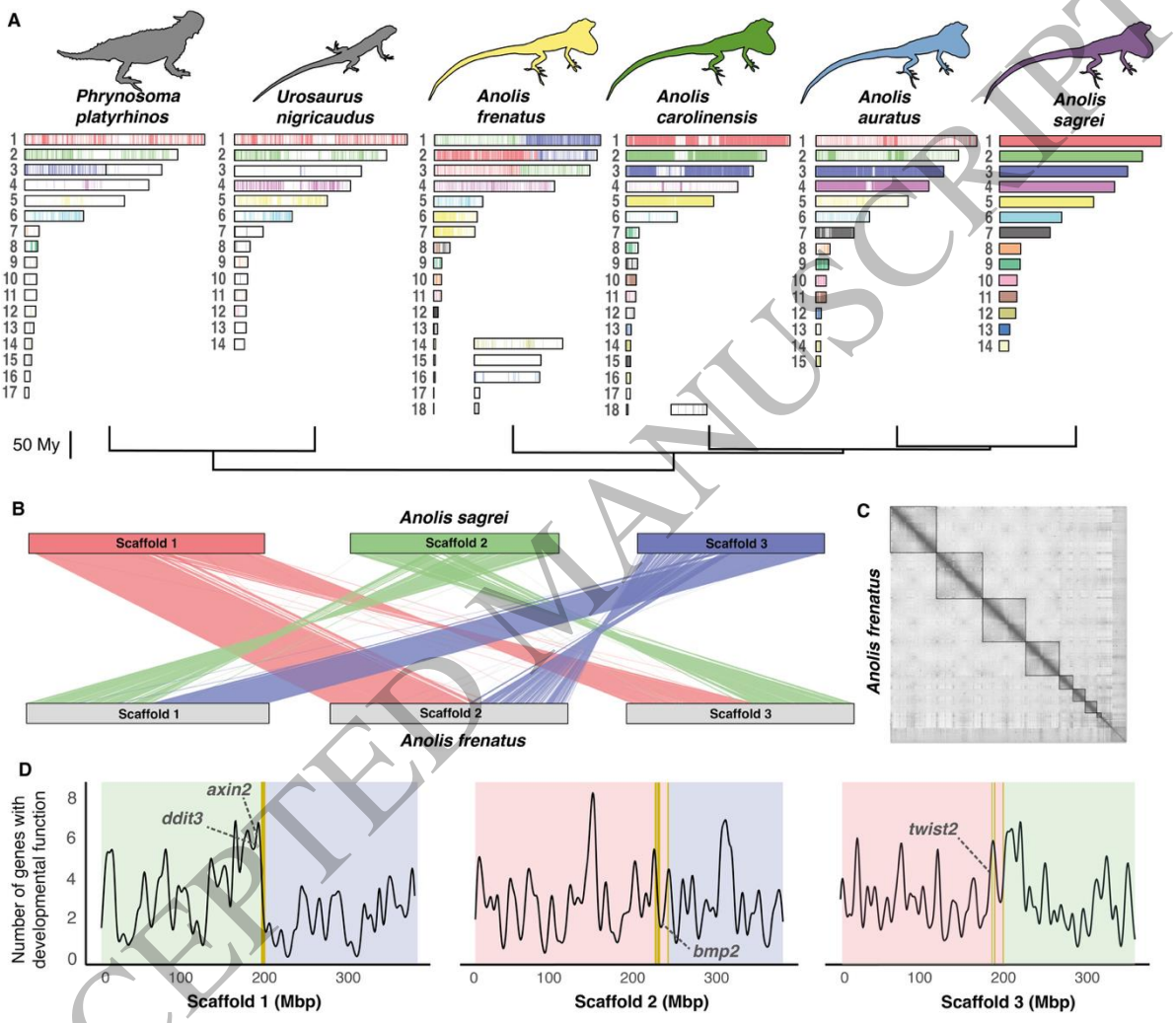

Figure 2. Chromosome-level structural variation across *Anolis*. **A.** Synteny between *A. sagrei* and other anole (*A. auratus*, *A. carolinensis*, *A. frenatus*) and lizard (*U. nigricaudus*, *P. platyrhinos*) species for the largest scaffolds representing the chromosomes of each species. **B.** Synteny between scaffolds 1, 2, and 3 of *A. sagrei* and *A. frenatus* showing substantial rearrangements. **C.** Hi-C density contact matrix for *A. frenatus*. **D.** Density of genes associated with developmental GO terms along scaffolds 1, 2 and 3 in *A. frenatus*.

Background colors indicate the homology to *A. sagrei* scaffolds for different chromosomal regions and vertical lines indicate the chromosomal breakpoints. Rearrangement breakpoints are within hotspots of developmental genes.

Scaffold 7 in *A. sagrei* has previously been hypothesized to be the X chromosome and the result of a series of autosomal fusions (Geneva et al. 2022; Giovannotti et al. 2017; Kichigin et al. 2016). *A. auratus* and *A. sagrei* belong to the *Norops* clade of *Anolis* (Poe et al. 2017). We found a high degree of synteny conservation between scaffold 7 of these two species, whereas in the species outside of the *Norops* clade it corresponded to a series of smaller scaffolds (Fig. 2A, Fig. S3). To further explore scaffold 7 evolution within anoles we compared this chromosome against another recently published *Norops* clade high-quality genome, *A. apletophallus* (Pirani et al. 2023), which also revealed high synteny conservation with both *A. sagrei* and *A. auratus* (Fig. S3).

Repeat density is associated with key developmental genes in Anolis *and other pleurodonts*

The relative composition of repeat elements differed among species, as anoles have a higher proportion of DNA transposons and LINEs, whereas phrynosomatids have a relatively higher proportion of LTRs (Table S6; Fig. S4). We estimated the density of repeats in 500 kb windows throughout the first 6 scaffolds of *A. frenatus*, *A. auratus*, *A. sagrei*, *U. nigricaudus* and *P. platyrhinos*. We selected the densest repeat regions corresponding to the top 5% of repeat density and identified the genes present in those regions from our annotations (Table S7). For all species, the composition of repeats within repeat-rich regions did not differ significantly from the relative abundance of repeat

elements in scaffolds 1 through 6 (Table S6). Within these regions, in all the analyzed species we detected some developmental genes (Fig. 3) such as the *hoxB*, *hoxC*, and *hoxD* gene clusters, key determinants of the vertebrate body plan (Mallo 2018); *notch4*, a member of the NOTCH receptors family that are crucial for development (James et al. 2014); and *fgf11*, member of the fibroblast growth factor (FGF) family which are involved in development and morphogenesis (Tejedor et al. 2020). An enrichment analysis was conducted on the lists of genes located within these high repeat-density regions for each species with g:Profiler. Genes associated with regulatory and developmental biological processes (e.g. “developmental process”, “anatomical structure development”, “animal organ development”) were significantly overrepresented in the high repeat-density regions for all species (Table S8; Fig. S5).

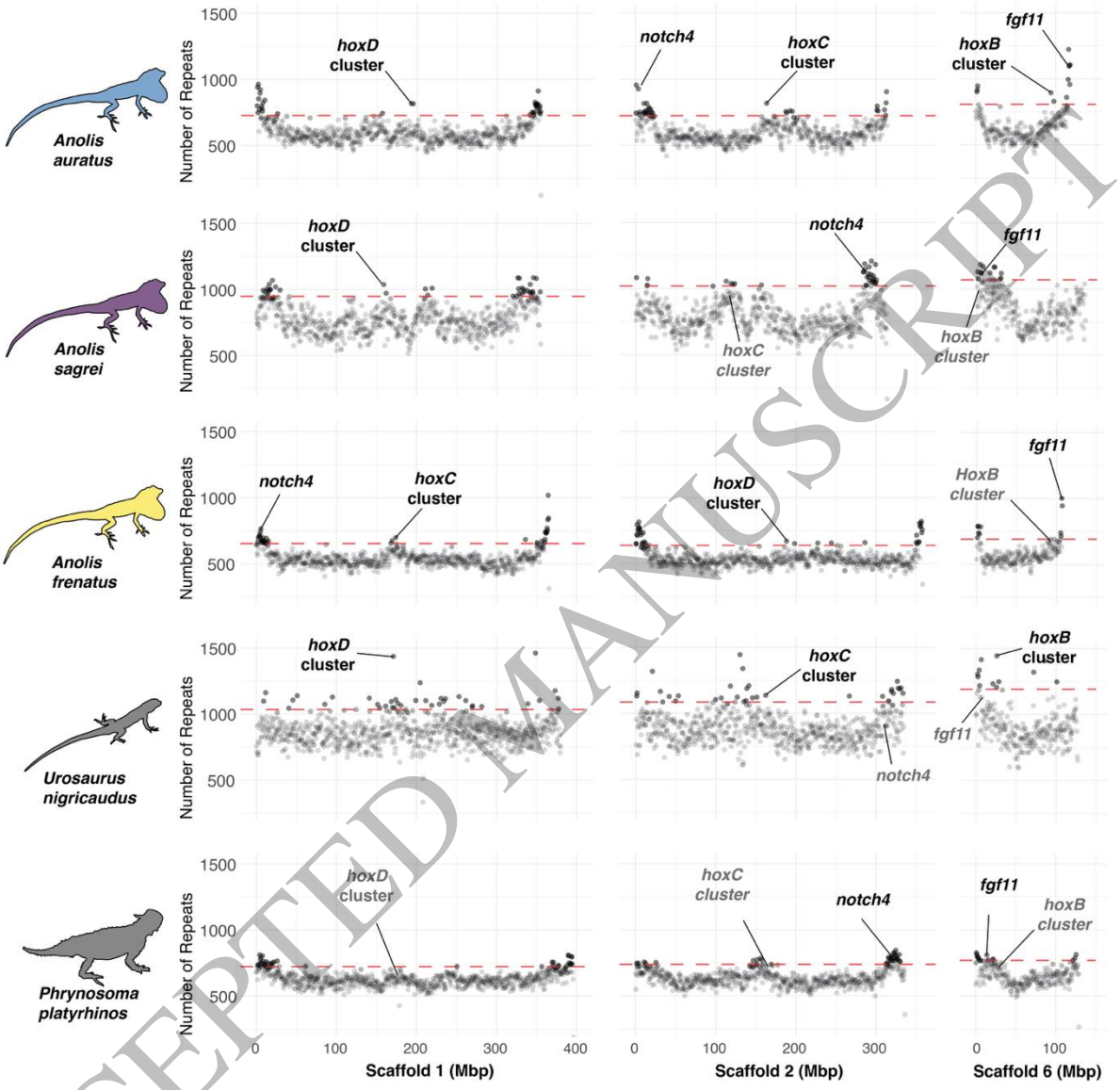

Figure 3. Number of repeat elements in 500 kb windows throughout scaffolds 1, 2 and 6 in the analyzed pleurodont species. A higher density of repeats is found close to key developmental genes in the four *Anolis* and the outgroups.

Genes potentially under natural selection and divergence in regulatory regions

As an approach to identify potential genes under selection, we calculated the pairwise ratio between non-synonymous to synonymous substitutions (dN/dS) for all genes between each species pair for the analyzed *Anolis* species (Table S9). We retained genes with dN/dS > 1 overlapping in at least 2 out of 3 comparisons for each species (Fig. S6). For *A. frenatus* 16 genes overlapped including *mtpn*, a muscle growth factor that shows similar effects to *igf1* (Hayashi 2001; Mohammadabadi et al. 2021); and *pdzk1ip1* that regulates and inhibits transforming growth factor (TGF-β) and bone morphogenic protein (BMP) signaling (Ikeno et al. 2019). For *A. auratus* 12 genes overlapped including *ramp2* which regulates angiogenesis, cardiovascular development, and influences bone formation (Naot & Cornish 2008; Shindo et al. 2019); and *dcdc1*, associated with bone mineral density (the Genetic Factors for Osteoporosis (GEFOS) Consortium 2009) and bone degradation in humans (Rossi et al. 2020). In *A. carolinensis* we detected 6 overlapping genes including *lep*, a gene relevant to lipid metabolism and energetic balance, and that has thermogenic effects on skeletal muscle (Dulloo et al. 2002; Fischer et al. 2020; Kaiyala et al. 2016); *clps*, involved in lipid digestion (Brockman 2002); and *stard6*, associated with the intracellular transport of sterol and other lipids (Soccio et al. 2002). *Anolis sagrei* presented 8 overlapping genes including *ppdpf1*, associated with cell proliferation in multiple types of cancer (Zheng et al. 2022); and *s100a1*, that can regulate cell growth and proliferation (Yu Zhang et al. 2021). A gene enrichment analysis was run with g:Profiler for each species (Table S10). Among the overrepresented GO terms for *A. carolinensis* we detected “lipid catabolic process” and “digestion”, for *A. auratus* “positive regulation of developmental processes”, for *A. frenatus* “regulation of muscle organ development”, and for *A. sagrei* “regulation of polarized epithelial cell differentiation”.

To identify diverged regulatory regions, we identified genes with the top 1% of divergence in their putative promoter regions (1,000 bp upstream of the transcription start site, (Andersson & Sandelin 2020) for each species pair (Table S11). We retained genes that overlapped in at least 2 out of 3 species comparisons. Within the overlapping genes identified for *A. frenatus* we found *wnt4*, key ligand of Wnt/β-catenin signaling that controls development and cell differentiation (Quanlong Zhang et al. 2021); *traf4*, an important regulator of embryogenesis and bone development (Li et al. 2019); *hspg2*, which influences skeletal and cardiovascular development (Martinez et al. 2018); and *errfi1*, that affects cell growth by regulating EGFR signaling (Cairns et al. 2018). In *A. carolinensis* we detected genes associated with lipid metabolism like *plin3*, *lpin1*, *ncoa1* (Csaki et al. 2013; Wagner et al. 2021; Zhu et al. 2019). For *A. auratus* we found *cib2*, associated with mechanoelectrical transduction in auditory cells (Wang et al. 2017). In *A. sagrei* we found *rab3d* involved in bone resorption (Zhu et al. 2016); and *optn*, a gene associated with autoimmune and neurodegenerative disorders (Mou et al. 2022).

We combined these genes with high divergence in the regulatory regions with the genes previously identified with dN/dS > 1 to generate our candidate gene set. We then used STRING v11 (Szklarczyk et al. 2019) to estimate gene interaction networks for genes in our combined candidate set to obtain an integrative view of evolutionary processes that spanned both regulatory and protein divergence (Fig. 4A). Some genes with dN/dS > 1 were embedded within gene interaction networks of genes with high divergence in regulatory regions (Fig. 4A, Fig. S7). For example, in *A. carolinensis* several genes in the gene interaction network have functions associated with gene regulation, lipid metabolism, and mitochondria (Fig. 4A). The positively selected *lep* gene constitutes a central node in

the gene interaction network and interacts with other elements of similar function that present high divergence in the regulatory regions.

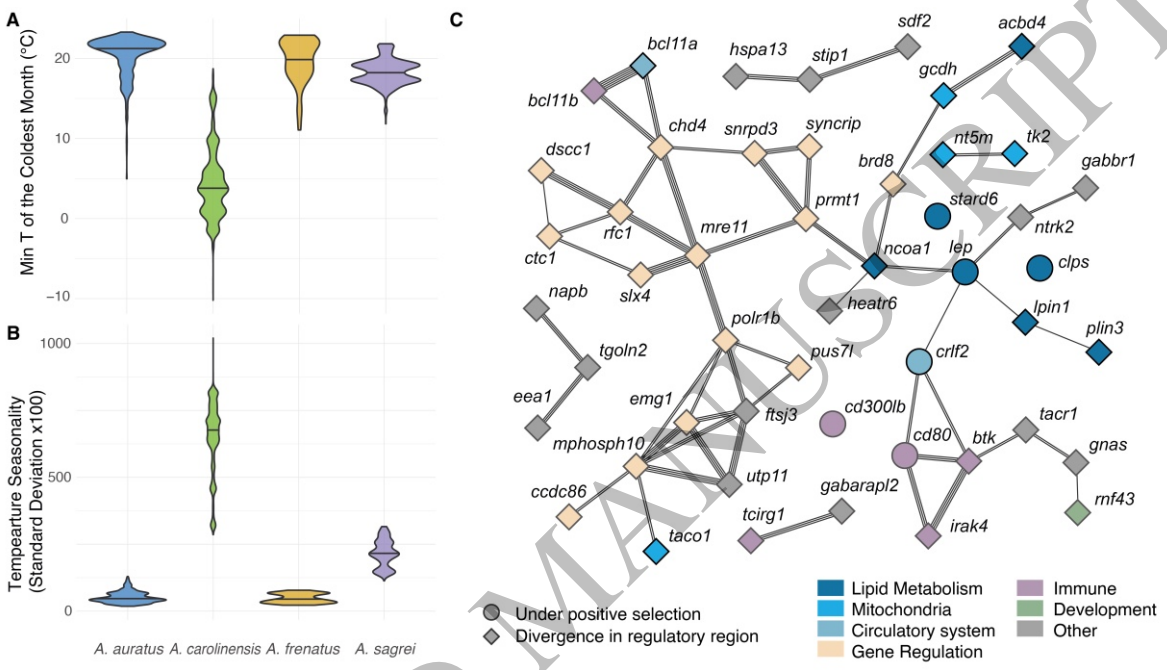

Figure 4. Climatic niche characterization across the native distribution range of the four studied anole species. **A.** Gene interaction network for the genes with dN/dS > 1 and genes with high divergence on the promoter region for *A. carolinensis*. Line thickness represents the number of multiple evidence supporting the interaction between two genes. **B.** Minimum temperature of the coldest month. **C.** Temperature seasonality. *A. carolinensis* is the species inhabiting the coldest and more thermally seasonal environments.

Association with phenotypic traits

We characterized the realized climatic niche across the native distribution for the four *Anolis* species and detected that they have different climatic niches (Fig. S8). Among them, *A. carolinensis* occupies the coldest (Fig. 4B) and most thermally seasonal (Fig. 4C) environments. This is in accordance with genes with dN/dS > 1 and regulatory divergence mostly associated with biological functions that could influence cold tolerance such as lipid metabolism, mitochondrial function, and circulatory system (Fig. 4A).

The morphology of the four focal species was also analyzed (Fig. S9). *Anolis frenatus* is distinct in its larger body size (Fig. 5A). The genes *mtpn* and *pdzk1ip1* had dN/dS > 1 in *A. frenatus* with respect to the other three species and could influence its larger body size (Fig. 5C). In contrast, *A. auratus* is characterized by its unique tail elongation (Fig. 5B). We explored the morphology of the caudal vertebrae, and we found that the long tail in *A. auratus* is achieved by an elongation of the caudal vertebrae rather than an increase in the number of vertebrae when compared to the other species (Fig. 5D). The relative length of the trunk vertebrae of *A. auratus* did not differ from the other species (Fig. S10). *Anolis frenatus* also features a relatively longer tail and longer caudal vertebrae than *A. sagrei* and *A. carolinensis*, but not as long as *A. auratus* (Fig. 5D). Among the genes with dN/dS > 1 in *A. auratus* we detected *ramp2* and *dcdc1*, which could be associated with the vertebral elongation phenotype (Fig. 5E).

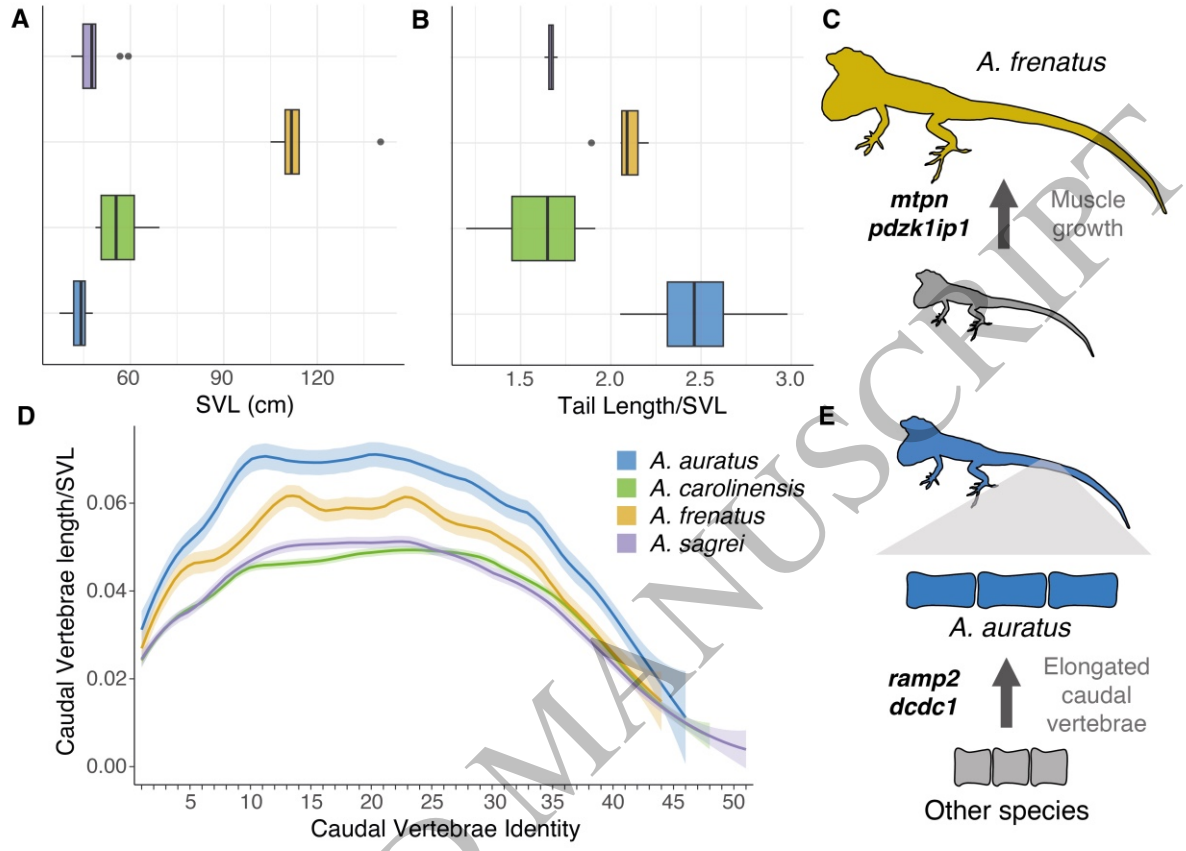

Figure 5. Morphological variation in distinctive traits of the analyzed species. **A.** *A. frenatus* stands out for its large body size. **B.** *A. auratus* its characterized by a long tail. **C.** Selection on the *mtpn* and *pdzk1ip1* genes could influence *A. frenatus* body size. **D.** The long tail in *A. auratus* is caused by an elongation of the caudal vertebrae rather than the addition of more vertebrae. **E.** Selection on *ramp2* and *dcdc1* could influence the vertebral elongation in *A. auratus*.

Discussion

Genomic characteristics can influence speciation and promote phenotypic variation within adaptive radiations (Gillespie et al. 2020; Marques et al. 2019). Here, we explored the genomic variation, namely chromosomal rearrangements and repeat element concentration, potentially contributing to diversity and phenotypic disparity within the *Anolis* radiation. Our results show examples of major structural rearrangements, high densities of TEs around developmental genes, and potential signatures of natural selection and divergence on regulatory regions that enable the formulation of hypothesis of the mechanisms that affect the unique phenotypes in these *Anolis* species.

Major structural rearrangements within Anolis

Chromosome-level structural variations can directly influence speciation by disrupting meiosis in heterozygotes and reducing fertility in hybrids or generating barriers to gene flow (Lucek et al. 2023; Olmo 2005). Moreover, they can modify the gene regulation and recombination patterns (Damas et al. 2021; Mérot et al. 2020). Our synteny analysis detected major chromosomal rearrangements within *Anolis*. Chromosome fissions and fusions have been previously described as highly relevant in anoles (Castiglia et al. 2013; Gamble et al. 2014), but we also identified some translocations, inversions, and deletions among the analyzed species.

Chromosomes 1, 2 and 3 presented a substantial rearrangement in *A. frenatus* (Fig. 2B). Hi-C analysis suggests this is a true rearrangement and not a technical artifact given that contact maps show strong within-chromosome interactions and little to no interactions between these chromosomes (Fig. 2C, Fig. S2). In general, squamates show high synteny

conservation for the major chromosomes (Davalos-Dehullu et al. 2023; Koochekian et al. 2022), and this result shows that at least one anole species deviates from the pattern. *Anolis frenatus* is part of the deeply divergent *Dactyloa* clade of *Anolis* (Fig. 1A; (Poe et al. 2017), and with our current sampling we cannot determine if this mutation evolved uniquely in *A. frenatus* or is common to other species within *Dactyloa*. Chromosomes 1, 2, and 3 are bigger in other *Dactyloa* anoles when compared to non-*Dactyloa* karyotypes (Table S12), but a detailed genomic analysis including other species from the clade would be needed to determine the origin of this mutation. Nonetheless, the chromosomal breaks in *A. frenatus* were located in areas with a high density of genes with developmental functions (Fig. 2D), including some genes highly relevant to skeletal and muscle development and growth like *axin2*, *bmp2*, *ddit3*, and *twist2* (Dao et al. 2010; Liu et al. 2017; Shu et al. 2011; Zecchini et al. 2019). The major structural rearrangements could have altered the gene regulation patterns of these developmental genes adjacent to them (Damas et al. 2021; Mérot et al. 2020). This allows us to hypotesize that the structural rearrangements in *A. frenatus* (and potentially other *Dactyloa*) could have influenced the evolution of body size and morphology.

Our results also allowed us to explore patterns of sex chromosome evolution across *Anolis*. Anoles share a single ancestral XY sex chromosome system but have commonly experienced chromosomal fission and fusion, including fusions that involve sex chromosomes (Gamble et al. 2014; Rovatsos et al. 2014). In *A. sagrei* the X chromosome (scaffold 7) has been reported as the fusion of chromosomes 9, 12, 13 and 18 from *A. carolinensis* (Geneva et al. 2022; Giovannotti et al. 2017; Kichigin et al. 2016). Further, Giovannotti et al. (Giovannotti et al. 2017) described chromosome 7 homology between *A.*

sagrei and *A. valencienni*, both belonging to the *Norops* clade of anoles. Our results are consistent with this finding (Fig. 2A; Fig. S3) and expand the homology for the sex chromosome to all three analyzed *Norops*-clade anoles (*A. auratus*, *A. apletophallus* and *A. sagrei*), with only within-chromosome structural changes such as inversions and deletions differing among these species (Fig. S3). *Norops* is one of the most diverse clades within *Anolis* (Poe et al. 2017) with ~200 species. Our findings suggest that the X-autosome fusions detected in *Anolis sagrei* arose early in the clade (~40 Mya; Fig. 1), and highlight the relevance of sex chromosome evolution for anole diversification (Gamble et al. 2014; Rovatsos et al. 2014).

Key developmental genes in repeat-rich regions in Anolis *and other pleurodonts.*

Repeat elements can be a source of genetic variation because they can modify gene regulation patterns, be a source of mutations, and trigger structural rearrangements (Bourque et al. 2018; Schrader & Schmitz 2019). The genome-wide percentage of repeats was similar among species (Table 1), but *A. carolinensis* had a lower percentage of repeats, potentially due to the comparatively less complete and contiguous assembly currently available for this species (Alföldi et al. 2011). The relative composition of repeat families differed among genera, with anoles characterized by a higher abundance of DNA transposons and LINEs (Fig. S4)(as previously reported; Feiner 2019; Gable et al. 2023). Moreover, we found a high density of repeats associated with key developmental genes such as *notch4*, *fgf11*, and the *hoxB*, *hoxC* and *hoxD* clusters in *Anolis* and the outgroups (Fig. 3; James et al. 2014; Mallo 2020; Tejedor et al. 2020). An enrichment analysis detected that genes located in repeat-rich regions were mostly associated with

developmental and regulatory functions (Fig. S4, Table S6). For all analyzed species, the composition of repeat families within repeat-rich regions did not differ from their genome-wide relative abundance (Table S4). This suggests that the patterns of repeat accumulation are not biased toward a specific class of repeats. Other gene families, such as the major histocompatibility complex (MHC), have also been described to show a higher abundance of repeats in anoles versus other squamates (Card et al. 2022).

Feiner (Feiner 2016, 2019) reported this unique pattern of repeat accumulation around the *hox* gene clusters in anoles, whereas other more distantly related squamates have a significantly lower number of repeats in these regions. Those studies, however, did not include other pleurodont lizards such as the phrynosomatids *U. nigricaudus* and *P. platyrhinos*. Thus, our analysis expands the pattern of repeat element accumulation to other genes that also affect development (Table S5) and indicates that this is not a feature exclusive to *Anolis* but is also present in other species from the Pleurodonta clade of Iguania. Pleurodont lizards include some of the most diverse vertebrate genera with respect to species number and morphological variation (e.g. *Anolis*, *Liolaemus*, *Sceloporus*; Alencar et al. 2024; Blankers et al. 2013). Therefore, the accumulation of repeat elements around developmental genes could be a source of genetic variation that fueled morphological innovation in pleurodont groups (Feiner 2019). Exploring the potential effects of the repeat accumulation on genetic and phenotypic variation for these lizard groups is key to understanding whether TE dynamics contribute to their evolvability and diversification. However, additional genomes assembled from within pleurodonts and other iguanians are needed to identify specifically when this pattern arose.

Potential signatures of selection on coding regions and regulatory divergence could influence unique phenotypes in Anolis

For the analyzed species we detected some candidate genes potentially under selection and genes with high divergence in their regulatory regions that we can hypothesize to influence their unique phenotypes (Fig. 4, Fig. S7). While phylogenetically explicit methods could provide better insight into the lineage-specific signatures of selection given the lack of evolutionary independence among our samples, we focused on pairwise comparisons because our heavily underrepresented sampling of the anole diversity (four out of over 400 species) could bias comparative analyses (Boettiger et al. 2012). Moreover, we acknowledge that our approach has more power to identify signatures of pervasive selection rather than episodic selection. Future work, combining more comprehensive sampling within *Anolis* with estimates of selection using a phylogenetic approach, has the potential to provide further, powerful insights into the evolutionary dynamics of the genus.

Anolis carolinensis presented dN/dS > 1 and high regulatory divergence on genes potentially influencing cold adaptation. In general, ectotherm adaptation to cold environments involves physiological processes of oxygen consumption and blood circulation (Angilletta Jr. 2009; Campbell-Staton et al. 2018). Among the genes under selection in *A. carolinensis*, leptin (*lep*) was a central node in the gene interaction network (Fig. 4). Moreover, other genes associated with lipid metabolism (e.g. *clps*, *stard6*, *ncoa1*, *lpin1*, *plin3*) were also identified in our analysis. Lipid metabolism has been proposed as a potential thermal adaptation in ectotherms (Wollenberg Valero et al. 2014). For instance, it could be an alternative energy source during cold seasons with lower resource availability (Sun et al. 2022), or it could be associated with changes in cell membrane composition

impacting fluidity in colder temperatures (Seebacher et al. 2009). Genes associated with lipid metabolism have been identified as undergoing accelerated evolution when comparing Cuban anole species with different thermal biology (Sakamoto et al. 2024). Furthermore, genes interacting with leptin and involved in lipid metabolism have been identified as under-selection in *A. cybotes* populations inhabiting cold high-elevation environments (Rodríguez et al. 2017). Therefore, it is possible that changes in lipid metabolism could constitute an adaptation to cold environments in *A. carolinensis*. We also detected divergence in the regulatory region of genes associated with the circulatory system and mitochondria (Fig. 4). Populations of *A. carolinensis* inhabiting colder environments show lower oxygen consumption rates, and signatures of selection and changes in the expression of genes associated with the circulatory system (Campbell-Staton et al. 2016, 2018). Thus, changes in these genes could enhance oxygen intake for low oxygen availability under cold temperatures in *A. carolinensis* versus other anole species.

A. auratus stands out for its long tail. This species is usually found on the grass in dense vegetation patches, and a long tail may provide better balance when walking or jumping across narrow perches (Gillis et al. 2009; Hsieh 2015). Body elongation is a convergent phenotype in several reptiles, and most species develop longer bodies through the addition of vertebrae (Bergmann & Morinaga 2019). However, the extremely long tail in *A. auratus* is achieved by elongation of the caudal vertebrae rather than the addition of more segments (Fig. 5D). The longest caudal vertebrae in *A. auratus* are located distal to the ninth caudal vertebrae (e.g., Ca10-21, Fig. 5D). In anoles, the *m. caudofemoralis longus* originates from the proximal caudal vertebrae (e.g. Ca2-8 in *A. sagrei*, Herrel et al. 2008; Ca2-9 in *A. heterodermus*, *A. tolimensis, and A. valencienni*, Herrel et al. 2008; Ríos-

Orjuela et al. 2020; and Ca3-8 in *A. carolinensis*, Ritzman et al. 2012). This primary hip joint extensor is essential for locomotion and may also assist with lateral flexion of the tail when the hindlimb is fixed (Ritzman et al. 2012). Therefore, caudal vertebral elongation in *A. auratus* is most pronounced in a region of the tail that is less functionally constrained. The pattern of caudal vertebrae elongation in *A. auratus* is similar to that seen in the tail of arboreal *Peromyscus maniculatus* (Kingsley et al. 2024), the cervical vertebrae of giraffes (Agaba et al. 2016), the trunk of some plethodontid salamanders (Parra-Olea & Wake 2001) and some fish species (Ward & Mehta 2010). Among the mechanisms that could determine caudal vertebral elongation are genes associated with axial development and determinants of the caudal region such as the *hox13* genes, *fgf8*, or *fgfr1* (Agaba et al. 2016; Kingsley et al. 2024; Mallo 2018, 2020; Ye & Kimelman 2020). Nonetheless, genes positively selected in giraffes did not show dN/dS > 1 in *A. auratus* (Fig. S11). In our genetic data, we detected dN/dS > 1 in *ramp2* and *dcdc1*, which influence bone development (Naot & Cornish 2008; the Genetic Factors for Osteoporosis (GEFOS) Consortium 2009). Heterozygote knockout mice for *ramp2* present skeletal abnormalities such as lower bone density and delayed development of the lumbar vertebrae, producing a similar pattern of vertebral elongation (Kadmiel et al. 2011). In *Peromyscus maniculatus*, *dcdc1* is located within a locus associated with tail length (Kingsley et al. 2024). Thus, the mutations in these genes could contribute to the unique tail phenotype in *A. auratus*.

Finally, *A. frenatus* is characterized by a large body size and relatively long limbs. In general, vertebrate body size is determined by genes associated with insulin growth factors and growth hormone pathways (Beatty & Schwartz 2020; Kemper et al. 2012; Rotwein 2018; Silva et al. 2023). Our analysis identified some candidate genes potentially

associated with large body size in *A. frenatus*. We detected dN/dS > 1 on the *mtpn* and *pdzk1ip1* genes, both involved in muscle development, growth, and morphogenesis (Hayashi 2001; Ikeno et al. 2019; Massagué 2012; Mohammadabadi et al. 2021; Wang et al. 2014). Injection of *mtpn* in mice produces increased body and muscle weights (Shiraishi et al. 2006). Moreover, among the genes that presented high divergence in regulatory regions for *A. frenatus* we identified other genes highly relevant for development. For instance, *wnt4* can be modulated by the growth hormone (Vouyovitch et al. 2016), and mice with overexpression of *wnt4* present dwarfism (Lee & Behringer 2007). Further, knockout mice for *traf4* show reduced body weight than wildtype mice (Shiels et al. 2000). We interpret these results with caution because, given the phylogenetic distance between *A. frenatus* and the other study species, we cannot be certain whether these mutations are exclusive to *A. frenatus* or could be shared with other *Dactyloa* anoles.

Overall, the genes with dN/dS > 1 and with high divergence in their regulatory regions perform relevant biological functions that could affect the phenotypes of the analyzed species. This indicates that the combination of mechanisms acting at different hierarchical levels can aid in the generation of adaptive phenotypes in anoles. Changes in regulatory regions could provide more evolvability than changes in protein-coding sequences that are in general more constrained to mutations given their biological function (Hill et al. 2021; Sakamoto et al. 2024). Therefore, exploring the effects of regulatory sequence divergence and regulatory RNAs on gene expression and their impacts on species traits is key to understanding how this variation could promote anole phenotypic diversity.

Conclusions

Our analysis of novel genome assemblies of four anole species constitutes an early step to identifying the genomic variation that could contribute to the extensive phenotypic disparity among *Anolis* species. In *Anolis*, chromosome-level structural rearrangements could directly generate reproductive isolation and affect the gene regulation patterns of genes relevant to development and morphological configuration. Further, a high density of repeat elements close to key developmental genes could also contribute to variation in the expression of such genes. Finally, natural selection on few coding sequences but relevant to species traits, in addition to divergence in regulatory regions could also play a role in shaping phenotypic diversity. The interaction between these genomic characteristics and selection pressures potentially enabled the evolution of disparate phenotypes within anoles, but further analysis of a wider sample of high-quality genomes would help to formally address this hypothesis. We highlight that besides ecological opportunity, the genomic architecture of organisms can also influence adaptive radiations.

Methods

Sampling and type specimens

The *A. auratus* specimen was collected in Gamboa, Panama, and the *A. frenatus* specimen in Soberania National Park, Panama (Collecting Permits: SE/A-33-11 and SC/A-21-12, Autoridad Nacional de Ambiente, ANAM, Republic of Panama; IACUC Protocol: 2011-0616-2014-07 Smithsonian Tropical Research Institute). Additional samples of *A. carolinensis* and *A. sagrei* obtained from the Sullivan Company (Nashville, TN) and Marcus Cantos Reptiles (Fort Myers, FL) were included for morphological analyses

(IACUC Protocol: Arizona State University 19-1053R and 12-1247R). Table S1 shows the number of individuals collected per species and locations used for reference genome assemblies and morphological analyses. Specimens were euthanized by intracoelomic injection of sodium pentobarbital (IACUC Protocols 09-1053R, 12-1274R, and 15-1416R ASU). The type specimens for the *A. auratus* and *A. frenatus* reference genomes corresponded to adult females.

Reference Genomes

We generated new reference genomes for *A. auratus* and *A. frenatus*. Skeletal muscle from the *A. auratus* type specimen, and liver and heart from *A. frenatus* type specimen were sent for DNA extraction and whole genome sequencing. The RUC_Aaur_2 and RUC_Afre_2 genomes were sequenced by Dovetail Genomics on an Illumina PE150 platform, de novo assembled with meraculous v2.2.2.5 (Chapman et al. 2011). HiRise v2.1.6-072ca03871cc (Putnam et al. 2016) scaffolding was performed with Chicago and Hi-C chromatic conformation capture libraries. The published genome assemblies and annotations of *A. carolinensis* (AnoCar2.0, Alföldi et al. 2011; and Hi-C assembly from DNAzoo, Dudchenko et al. 2017, 2018) and *A. sagrei* (AnoSag2.1, Geneva et al. 2022) were included for comparative genomic analyses. Table 1 shows the assembly statistics for the four *Anolis* genomes. Additionally, we included the reference genome of the phrynosomatids *Phrynosoma platyrhinos* (MUOH_PhPlat_1.1, Koochekian et al. 2022) and *Urosaurus nigricaudus* (ASU_Uro_nig_1, Davalos-Dehullu et al. 2023) for some comparative genomic analyses.

A genome annotation was generated for *A. auratus* and *A. frenatus*. For each species, repeats were identified on the genome sequences by using RepeatModeler v2.0.1 (Flynn et al. 2020), and then repeat elements were soft-masked on the assembly with RepeatMasker v4.1.1 (Smit et al. 2015). To aid in annotation we generated a *de novo* transcriptome for each species using tail and ovary/yolk for *A. auratus* and brain and ovary for *A. frenatus*. Tissue samples were collected from the same animals used for genome sequencing. Tissues were sent to the Yale Center for Genomic Analyses (YCGA; West Haven, CT) for RNA extraction, cDNA poly-A-enriched Illumina library preparation and sequencing on an Illumina NovaSeq S4 platform using 150-bp paired end reads. Read quality was assessed with FastQC v0.11.7 (Andrews 2010), and reads were trimmed with Trimgalore v0.6.8 (Krueger 2015). Then a *de novo* transcriptome assembly was generated with Trinity v2.12.0 (Grabherr et al. 2011). The generated transcriptomes were used as evidence for each species genome annotation respectively.

Multiple iterations of Maker v3.01.03 (Campbell et al. 2014) were run to annotate the genomes. We used the species-specific transcripts, and the protein-coding sequences from *A. carolinensis* and *A. sagrei* as evidence. A first round of Maker was run for aligning and mapping transcript and protein evidence. Then, two additional rounds of *ab initio* gene model prediction using Augustus v3.4.0 (Stanke et al. 2006) and SNAP v2006-07-28 (Korf 2004) were run. After each round of Maker, the Annotation Edit Distance (AED) was recorded, and annotation completeness was assessed with BUSCO v5.4.2 (Simão et al. 2015) on the predicted transcripts obtained from Maker, comparing against the eukaryote and sauropsid gene datasets.

Chromosome-level structural rearrangements

We investigated synteny among the main scaffolds from the four analyzed *Anolis* species along with the phrynosomatids *P. platyrhinos* and *U. nigricaudus* by *in silico* chromosome painting. For this analysis, we used the high contiguity DNAzoo Hi-C-scaffolded genome assembly of *A. carolinensis* (Dudchenko et al. 2017, 2018). All species were compared against the *A. sagrei* genome as a reference, because it is the species with the most contiguous and complete genome among our samples (Geneva et al. 2022). The first 14 scaffolds from *A. sagrei*, representative of its chromosomes, were split in chunks of 100 bp with "faSplit" v438 from the UCSC Bioinformatic Utilities (Kuhn et al. 2013). Then, we used blastn v2.10.0 (Camacho et al. 2009) to map each fragment onto the 5 other species' genome. We retained matches with at least 50 bp length, and that were contiguous in at least 5 matches (Koochekian et al. 2022). To further explore the chromosome X evolution within *Anolis*, we compared chromosome 7 from *A. sagrei* to the closely related *A. apletophallus* (Pirani et al. 2023) following the same methodology.

Hi-C data analysis

Link density histograms were generated with Juicer v2.0 (Durand et al. 2016) by mapping paired reads from the Hi-C libraries for *A. auratus* and *A. frenatus* to the finished genome assembly to assess chromatin conformation and to validate our chromosomal rearrangements. Hi-C contact maps were visualized with Juicebox v1.9.8 (Dudchenko et al. 2018).

Developmental genes located in A. frenatus scaffolds 1, 2 and 3 rearrangement

We explored which genes were located adjected to the rearrangement among scaffolds 1, 2, and 3 detected between *A. frenatus* and *A. sagrei*. For this, we pulled from the *A. sagrei* annotation the genes located within 1 Mbp from the scaffold breakpoints identified with the synteny analysis. We performed an enrichment analysis on the genes located in these regions with g:Profiler ve111_eg58_p18_30541362 (Kolberg et al. 2023) to assess which biological processes were overrepresented in that gene list. Then, we extracted the list of genes present in scaffolds 1, 2, and 3 in *A. frenatus* to identify if the chromosomal breaks were located in hotspots of genes with developmental function. We identified and extracted all the GO terms included in the list of genes located on each scaffold with g:Profiler using *Homo sapiens* as a reference, and we retained only the genes matching GO terms that included any of the keywords: "development", "morpho", "growth" or "organ". We then calculated the number of genes with those developmental functions along each chromosome in 500 kbp windows in R v4.1.2 (R Core Team 2022) with a custom script.

Repeat density through the genomes

For *A. auratus*, *A. frenatus*, *A. sagrei*, *U. nigricaudus* and *P. platyrhinos* we calculated the repeat density for each one of the largest 6 scaffolds. First, we reclassified repeat families for the annotations of *U. nigricaudus*, *P. platyrhinos* and *A. sagrei*, following the same methodology used for *A. auratus* and *A. frenatus*. We compared the repeat family composition for the largest 6 scaffolds among the five species with a Fisher's exact test in R. Then, the number of repeats was calculated in 500 kbp windows, and we retained repeats

longer than 50 bp and with a score value over 10 (Feiner 2016). Then, we selected the 500 kbp windows corresponding to the highest 5% of repeat density per scaffold for each species with a custom script in R. To assess if those regions were enriched in a particular class of repeats, we compared the repeat family composition of the repeat-rich regions against the largest 6 scaffolds for each species with a Fisher's exact test. Then, we identified the genes located within those high repeat density regions using the respective genome annotations. An enrichment analysis was performed to identify the most represented gene ontology (GO) categories on the list of genes situated in high repeat regions for each species with g:Profiler, and the enriched GO terms were semantically organized and visualized with Revigo v1.8.1 (Supek et al. 2011).

Identification of genes potentially under positive selection and regulatory elements with high divergence

We looked for genes potentially under positive selection among the four *Anolis* species by calculating the ratio between non-synonymous to synonymous mutations (dN/dS) between orthologs from species pairs with the "orthologr" package (Drost et al. 2015) in R using the Comeron's (Comeron 1995) method. To identify genes with dN/dS > 1 in each species, we retained the genes overlapping in at least 2 out of 3 comparisons between the focal and the other three species. We focused on pairwise comparisons instead of phylogenetically explicit methods to detect genes under selection, because heavily underrepresented phylogenies could bias comparative analyses (Boettiger et al. 2012). Moreover, having fewer than 10 species significantly decreases the statistical power when using phylogeny-based approaches (Murrell et al. 2012). An enrichment analysis was performed on the list

of positively selected genes with g:Profiler to identify the most represented GO terms for each species, using *Homo sapiens* as a reference.

To assess regulatory regions with high divergence we focused on the 1000 kb upstream of the transcription start, which includes the promoter region (Andersson & Sandelin 2020). We compared orthologs between species pairs previously identified with "orthologr" in R. Each ortholog pair was aligned with mafft v7.520 (Katoh & Standley 2013) and the genetic distance between aligned orthologs was estimated with the "bio3d" package (Grant et al. 2006) in R. We considered the genes with the top 1% of genetic distance as genes with the highest divergence in their regulatory regions between species pairs. For each species we retained the genes overlapping in at least 2 out of 3 comparisons. Finally, we used STRING v12.0 (Szklarczyk et al. 2019) to evaluate gene interactions among the genes under selection and the genes with high regulatory divergence for each species.

Climatic niche analyses

For each species, occurrence records were obtained from the Global Biodiversity Information Facility (GBIF.Org 2021). Occurrences were deduplicated and manually curated to accurately represent the native distribution of each species. The final dataset included 881 occurrences for *A. auratus*, 175 for *A. frenatus*, 27,546 for *A. carolinensis*, and 24,419 for *A. sagrei*. Raster data for the 19 bioclimatic variables with 1 km^2 of spatial resolution was obtained from the WorldClim v2 database (Fick & Hijmans 2017). For each occurrence point, the corresponding values of the 19 bioclimatic variables were obtained

using QGIS v3.16.16-Hannover (QGIS.org 2020). We qualitatively compared the climatic niche among the four analyzed species. Climatic variation was visualized with a Principal Component Analysis (PCA) in R, and the main variables differentiating species were identified based on their loadings in the first two principal components.

Morphological analyses

Additional samples for the four *Anolis* species were included for morphological analyses. Skeletal data was obtained from osteological preparations following Tollis et al. (2018) modification of amphibian protocols, or from micro-computed tomography (microCT) images collected in a Siemens Inveon micro-CT scanner at the RII Translational Bioimaging Resource at the University of Arizona (Table S2). For skeletal preparations, individuals were photographed with a scale in a stereodissecting microscope (Nikon SMZ800 with Coolpix 995 digital camera), and morphological traits were measured with ImageJ v1.53k (Schneider et al. 2012). For microCT scans, digital images were analyzed and measured with InVesalius v3.1.1 (Amorim et al. 2015). For each species we measured snout–vent length (SVL), axilla–groin distance (AGD), forelimb total length (FLL), forelimb autopod length, forelimb stylopod length, forelimb zeugopod length, hindlimb total length (HLL), hindlimb autopod length, hindlimb stylopod length, hindlimb zeugopod length, head width (HW), head length (HL), head height (HH) and tail length (TL). We also analyzed the osteology of the caudal vertebrae for the four *Anolis* species. For this, we measured the distance from the distal end of the cotyle to the proximal tip of the condyle on each caudal vertebra. All measurements apart from SVL were standardized by dividing by

the distance between the snout to the end of the sacral vertebrae as an approximation to body size. We compared microCT and skeletal preparation measurements with a paired T-test to assess possible bias in the sampling methodology (Table S13).

Data Availability

All raw read files have been accessioned to the NCBI SRA under BioProject #PRJNA1096315. Final genome assemblies and annotations have been accessioned to the Harvard Dataverse (https://doi.org/10.7910/DVN/F9NDWL).

Funding

This project was supported by funding from NSF grant DEB-1927194 to AJG and JL, DGE-2152059 to AJG, and the College of Liberal Arts and Sciences at Arizona State University (ASU) to KK. RAD was supported by the Doctoral scholarship 72200094 (ANID, Chile) and the Peabody Family Memorial Award. Support for EL was provided by the ASU School of Life Sciences Undergraduate Research Program.

References

Agaba M, Ishengoma E, Miller WC, McGrath BC, Hudson CN, et al. 2016. Giraffe genome sequence reveals clues to its unique morphology and physiology. Nat Commun. 7. doi: 10.1038/ncomms11519.

Alencar LRV, Schwery O, Gade MR, Domínguez-Guerrero SF, Tarimo E, et al. 2024. Opportunity begets opportunity to drive macroevolutionary dynamics of a diverse lizard radiation. Evolution Letters. doi: 10.1093/evlett/qrae022.

Alföldi J, Di Palma F, Grabherr M, Williams C, Kong L, et al. 2011. The genome of the green anole lizard and a comparative analysis with birds and mammals. Nature. 477:587–591. doi: 10.1038/nature10390.

Amorim P, Moraes T, Silva J, Pedrini H. 2015. InVesalius: An Interactive Rendering Framework for Health Care Support. In: Advances in Visual Computing. Bebis, G, Boyle, R, Parvin, B, Koracin, D, Pavlidis, I, et al., editors. Lecture Notes in Computer Science Vol. 9474 Springer International Publishing: Cham pp. 45–54. doi: 10.1007/978-3-319-27857-5_5.

Andersson R, Sandelin A. 2020. Determinants of enhancer and promoter activities of regulatory elements. Nat Rev Genet. 21:71–87. doi: 10.1038/s41576-019-0173-8.

Andrews S. 2010. FastQC: a quality control tool for high throughput sequence data.

Angilletta Jr. MJ. 2009. *Thermal Adaptation*. Oxford University Press doi: 10.1093/acprof:oso/9780198570875.001.1.

Beatty AE, Schwartz TS. 2020. Gene expression of the IGF hormones and IGF binding proteins across time and tissues in a model reptile. Physiological Genomics. 52:423–434. doi: 10.1152/physiolgenomics.00059.2020.

Bergmann PJ, Morinaga G. 2019. The convergent evolution of snake-like forms by divergent evolutionary pathways in squamate reptiles. Evolution. 73:481–496. doi: 10.1111/evo.13651.

Blankers T, Townsend TM, Pepe K, Reeder TW, Wiens JJ. 2013. Contrasting global-scale evolutionary radiations: phylogeny, diversification, and morphological evolution in the major clades of iguanian lizards: Global Radiations in Lizards. Biol J Linn Soc Lond. 108:127–143. doi: 10.1111/j.1095-8312.2012.01988.x.

Boettiger C, Coop G, Ralph P. 2012. Is your phylogeny informative? Measuring the power of comparative methods. Evolution. 66:2240–2251. doi: 10.1111/j.1558-5646.2011.01574.x.

Bourque G, Burns KH, Gehring M, Gorbunova V, Seluanov A, et al. 2018. Ten things you should know about transposable elements. Genome Biol. 19. doi: 10.1186/s13059-018-1577-z.

Brawand D, Wagner CE, Li YI, Malinsky M, Keller I, et al. 2014. The genomic substrate for adaptive radiation in African cichlid fish. Nature. 513:375–381. doi: 10.1038/nature13726.

Brockman H. 2002. Colipase-induced reorganization of interfaces as a regulator of lipolysis. Colloids and Surfaces B: Biointerfaces. 26:102–111. doi: 10.1016/s0927-7765(02)00031-0.

Butler MA, Sawyer SA, Losos JB. 2007. Sexual dimorphism and adaptive radiation in *Anolis* lizards. Nature. 447:202–205. doi: 10.1038/nature05774.

Cairns J, Fridley BL, Jenkins GD, Zhuang Y, Yu J, et al. 2018. Differential roles of ERRFI1 in EGFR and AKT pathway regulation affect cancer proliferation. EMBO Reports. 19. doi: 10.15252/embr.201744767.

Camacho C, Coulouris G, Avagyan V, Ma N, Papadopoulos J, et al. 2009. BLAST+: architecture and applications. BMC Bioinformatics. 10. doi: 10.1186/1471-2105-10-421.

Campbell MS, Holt C, Moore B, Yandell M. 2014. Genome Annotation and Curation Using MAKER and MAKER-P. CP in Bioinformatics. 48. doi: 10.1002/0471250953.bi0411s48.

Campbell-Staton SC, Bare A, Losos JB, Edwards SV, Cheviron ZA. 2018. Physiological and regulatory underpinnings of geographic variation in reptilian cold tolerance across a latitudinal cline. Molecular Ecology. 27:2243–2255. doi: 10.1111/mec.14580.

Campbell-Staton SC, Edwards SV, Losos JB. 2016. Climate-mediated adaptation after mainland colonization of an ancestrally subtropical island lizard, *Anolis carolinensis*. J of Evolutionary Biology. 29:2168–2180. doi: 10.1111/jeb.12935.

Card DC, Van Camp AG, Santonastaso T, Jensen-Seaman MI, Anthony NM, et al. 2022. Structure and evolution of the squamate major histocompatibility complex as revealed by two Anolis lizard genomes. Front. Genet. 13. doi: 10.3389/fgene.2022.979746.

Castiglia R, Flores-Villela O, Bezerra AMR, Muñoz A, Gornung E. 2013. Pattern of chromosomal changes in 'beta' *Anolis* (*Norops* group) (Squamata: Polychrotidae) depicted by an ancestral state analysis. Zool. Stud. 52. doi: 10.1186/1810-522x-52-60.

Chapman JA, Ho I, Sunkara S, Luo S, Schroth GP, et al. 2011. Meraculous: De Novo Genome Assembly with Short Paired-End Reads Salzberg, SL, editor. PLoS ONE. 6:e23501. doi: 10.1371/journal.pone.0023501.

Comeron JM. 1995. A method for estimating the numbers of synonymous and nonsynonymous substitutions per site. J Mol Evol. 41. doi: 10.1007/bf00173196.

Csaki LS, Dwyer JR, Fong LG, Tontonoz P, Young SG, et al. 2013. Lipins, lipinopathies, and the modulation of cellular lipid storage and signaling. Progress in Lipid Research. 52:305–316. doi: 10.1016/j.plipres.2013.04.001.

Damas J, Corbo M, Lewin HA. 2021. Vertebrate Chromosome Evolution. Annu. Rev. Anim. Biosci. 9:1–27. doi: 10.1146/annurev-animal-020518-114924.

Dao DY, Yang X, Flick LM, Chen D, Hilton MJ, et al. 2010. Axin2 regulates chondrocyte maturation and axial skeletal development. Journal Orthopaedic Research. 28:89–95. doi: 10.1002/jor.20954.

Davalos-Dehullu E, Baty SM, Fisher RN, Scott PA, Dolby GA, et al. 2023. Chromosome-Level Genome Assembly of the Blacktail Brush Lizard, *Urosaurus nigricaudus*, Reveals

Dosage Compensation in an Endemic Lizard Mank, J, editor. Genome Biology and Evolution. 15. doi: 10.1093/gbe/evad210.

Di-Poï N, Montoya-Burgos JI, Miller H, Pourquié O, Milinkovitch MC, et al. 2010. Changes in Hox genes' structure and function during the evolution of the squamate body plan. Nature. 464:99–103. doi: 10.1038/nature08789.

Drost H-G, Gabel A, Grosse I, Quint M. 2015. Evidence for Active Maintenance of Phylotranscriptomic Hourglass Patterns in Animal and Plant Embryogenesis. Molecular Biology and Evolution. 32:1221–1231. doi: 10.1093/molbev/msv012.

Dudchenko O, Batra SS, Omer AD, Nyquist SK, Hoeger M, et al. 2017. De novo assembly of the *Aedes aegypti* genome using Hi-C yields chromosome-length scaffolds. Science. 356:92–95. doi: 10.1126/science.aal3327.

Dudchenko O, Shamim MS, Batra SS, Durand NC, Musial NT, et al. 2018. The Juicebox Assembly Tools module facilitates*de novo*assembly of mammalian genomes with chromosome-length scaffolds for under $1000. doi: 10.1101/254797.

Dulloo AG, Stock MJ, Solinas G, Boss O, Montani J-P, et al. 2002. Leptin directly stimulates thermogenesis in skeletal muscle. FEBS Letters. 515:109–113. doi: 10.1016/s0014-5793(02)02449-3.

Duncan CA, Cohick WS, John-Alder HB. 2020. Testosterone Reduces Growth and Hepatic *IGF-1* mRNA in a Female-Larger Lizard, *Sceloporus undulatus*: Evidence of an Evolutionary Reversal in Growth Regulation. Integrative Organismal Biology. 2. doi: 10.1093/iob/obaa036.

Durand NC, Shamim MS, Machol I, Rao SSP, Huntley MH, et al. 2016. Juicer Provides a One-Click System for Analyzing Loop-Resolution Hi-C Experiments. Cell Systems. 3:95–98. doi: 10.1016/j.cels.2016.07.002.

Edelman NB, Frandsen PB, Miyagi M, Clavijo B, Davey J, et al. 2019. Genomic architecture and introgression shape a butterfly radiation. Science. 366:594–599. doi: 10.1126/science.aaw2090.

Farleigh K, Ascanio A, Farleigh ME, Schield DR, Card DC, et al. 2023. Signals of differential introgression in the genome of natural hybrids of Caribbean anoles. Molecular Ecology. 32:6000–6017. doi: 10.1111/mec.17170.

Feiner N. 2016. Accumulation of transposable elements in *Hox* gene clusters during adaptive radiation o f*Anolis* lizards. Proc. R. Soc. B. 283:20161555. doi: 10.1098/rspb.2016.1555.

Feiner N. 2019. Evolutionary lability in *Hox* cluster structure and gene expression in *Anolis* lizards. Evolution Letters. 3:474–484. doi: 10.1002/evl3.131.

Fick SE, Hijmans RJ. 2017. WorldClim 2: new 1-km spatial resolution climate surfaces for global land areas. Intl Journal of Climatology. 37:4302–4315. doi: 10.1002/joc.5086.

Fischer AW, Cannon B, Nedergaard J. 2020. Leptin: Is It Thermogenic? Endocrine Reviews. 41:232–260. doi: 10.1210/endrev/bnz016.

Flynn JM, Hubley R, Goubert C, Rosen J, Clark AG, et al. 2020. RepeatModeler2 for automated genomic discovery of transposable element families. Proc. Natl. Acad. Sci. U.S.A. 117:9451–9457. doi: 10.1073/pnas.1921046117.

Gable SM, Mendez JM, Bushroe NA, Wilson A, Byars MI, et al. 2023. The State of Squamate Genomics: Past, Present, and Future of Genome Research in the Most Speciose Terrestrial Vertebrate Order. Genes. 14:1387. doi: 10.3390/genes14071387.

Gamble T, Geneva AJ, Glor RE, Zarkower D. 2014. *Anolis* Sex Chromosomes Are Derived from a Single Ancestral Pair. Evolution. 68:1027–1041. doi: 10.1111/evo.12328.

GBIF.Org. 2021. Occurrence Download. 29298189. doi: 10.15468/DL.TQHDNS.

Geneva AJ, Park S, Bock DG, De Mello PLH, Sarigol F, et al. 2022. Chromosome-scale genome assembly of the brown anole (*Anolis sagrei*), an emerging model species. Commun Biol. 5. doi: 10.1038/s42003-022-04074-5.

Gillespie RG, Bennett GM, De Meester L, Feder JL, Fleischer RC, et al. 2020. Comparing Adaptive Radiations Across Space, Time, and Taxa Murphy, W, editor. Journal of Heredity. 111:1–20. doi: 10.1093/jhered/esz064.

Gillis GB, Bonvini LA, Irschick DJ. 2009. Losing stability: tail loss and jumping in the arboreal lizard *Anolis carolinensis*. Journal of Experimental Biology. 212:604–609. doi: 10.1242/jeb.024349.

Giovannotti M, Trifonov VA, Paoletti A, Kichigin IG, O'Brien PCM, et al. 2017. New insights into sex chromosome evolution in anole lizards (Reptilia, Dactyloidae). Chromosoma. 126:245–260. doi: 10.1007/s00412-016-0585-6.

Grabherr MG, Haas BJ, Yassour M, Levin JZ, Thompson DA, et al. 2011. Full-length transcriptome assembly from RNA-Seq data without a reference genome. Nat Biotechnol. 29:644–652. doi: 10.1038/nbt.1883.

Grant BJ, Rodrigues APC, ElSawy KM, McCammon JA, Caves LSD. 2006. Bio3d: an R package for the comparative analysis of protein structures. Bioinformatics. 22:2695–2696. doi: 10.1093/bioinformatics/btl461.

Gunderson AR, Mahler DL, Leal M. 2018. Thermal niche evolution across replicated *Anolis* lizard adaptive radiations. Proc. R. Soc. B. 285:20172241. doi: 10.1098/rspb.2017.2241.

Han F, Lamichhaney S, Grant BR, Grant PR, Andersson L, et al. 2017. Gene flow, ancient polymorphism, and ecological adaptation shape the genomic landscape of divergence among Darwin's finches. Genome Res. 27:1004–1015. doi: 10.1101/gr.212522.116.

Hayashi T. 2001. S-myotrophin promotes the hypertrophy of myotube as insulin-like growth factor-I does. The International Journal of Biochemistry & Cell Biology. 33:831–838. doi: 10.1016/s1357-2725(01)00035-8.

Herrel A, Vanhooydonck B, Porck J, Irschick DJ. 2008. Anatomical Basis of Differences in Locomotor Behavior in *Anolis* Lizards: A Comparison Between Two Ecomorphs. Bulletin of the Museum of Comparative Zoology. 159:213–238. doi: 10.3099/0027-4100-159.4.213.

Hill MS, Vande Zande P, Wittkopp PJ. 2021. Molecular and evolutionary processes generating variation in gene expression. Nat Rev Genet. 22:203–215. doi: 10.1038/s41576-020-00304-w.

Hsieh ST. 2015. Tail loss and narrow surfaces decrease locomotor stability in the arboreal green anole lizard (*Anolis carolinensis*). Journal of Experimental Biology. doi: 10.1242/jeb.124958.

Huie JM, Prates I, Bell RC, De Queiroz K. 2021. Convergent patterns of adaptive radiation between island and mainland *Anolis* lizards. Biological Journal of the Linnean Society. 134:85–110. doi: 10.1093/biolinnean/blab072.

Ikeno S, Nakano N, Sano K, Minowa T, Sato W, et al. 2019. PDZK1-interacting protein 1 (PDZK1IP1) traps Smad4 protein and suppresses transforming growth factor-β (TGF-β) signaling. Journal of Biological Chemistry. 294:4966–4980. doi: 10.1074/jbc.ra118.004153.

James AC, Szot JO, Iyer K, Major JA, Pursglove SE, et al. 2014. Notch4 reveals a novel mechanism regulating Notch signal transduction. Biochimica et Biophysica Acta (BBA) - Molecular Cell Research. 1843:1272–1284. doi: 10.1016/j.bbamcr.2014.03.015.

Kadmiel M, Fritz-Six K, Pacharne S, Richards GO, Li M, et al. 2011. Research Resource: Haploinsufficiency of Receptor Activity-Modifying Protein-2 (Ramp2) Causes Reduced Fertility, Hyperprolactinemia, Skeletal Abnormalities, and Endocrine Dysfunction in Mice. Molecular Endocrinology. 25:1244–1253. doi: 10.1210/me.2010-0400.

Kaiyala KJ, Ogimoto K, Nelson JT, Muta K, Morton GJ. 2016. Physiological role for leptin in the control of thermal conductance. Molecular Metabolism. 5:892–902. doi: 10.1016/j.molmet.2016.07.005.

Kanamori S, Díaz LM, Cádiz A, Yamaguchi K, Shigenobu S, et al. 2022. Draft genome of six Cuban Anolis lizards and insights into genetic changes during their diversification. BMC Ecol Evo. 22:129. doi: 10.1186/s12862-022-02086-7.

Katoh K, Standley DM. 2013. MAFFT Multiple Sequence Alignment Software Version 7: Improvements in Performance and Usability. Molecular Biology and Evolution. 30:772–780. doi: 10.1093/molbev/mst010.

Kemper KE, Visscher PM, Goddard ME. 2012. Genetic architecture of body size in mammals. Genome Biology. 13:244. doi: 10.1186/gb-2012-13-4-244.

Kichigin IG, Giovannotti M, Makunin AI, Ng BL, Kabilov MR, et al. 2016. Evolutionary dynamics of Anolis sex chromosomes revealed by sequencing of flow sorting-derived microchromosome-specific DNA. Mol Genet Genomics. 291:1955–1966. doi: 10.1007/s00438-016-1230-z.

Kingsley EP, Hager ER, Lassance J-M, Turner KM, Harringmeyer OS, et al. 2024. Adaptive tail-length evolution in deer mice is associated with differential Hoxd13 expression in early development. Nat Ecol Evol. 8:791–805. doi: 10.1038/s41559-024-02346-3.

Kolberg L, Raudvere U, Kuzmin I, Adler P, Vilo J, et al. 2023. g:Profiler—interoperable web service for functional enrichment analysis and gene identifier mapping (2023 update). Nucleic Acids Research. 51:W207–W212. doi: 10.1093/nar/gkad347.

Koochekian N, Ascanio A, Farleigh K, Card DC, Schield DR, et al. 2022. A chromosome-level genome assembly and annotation of the desert horned lizard, *Phrynosoma platyrhinos*, provides insight into chromosomal rearrangements among reptiles. GigaScience. 11. doi: 10.1093/gigascience/giab098.

Korf I. 2004. Gene finding in novel genomes. BMC Bioinformatics. 5. doi: 10.1186/1471-2105-5-59.

Kozak KM, Joron M, McMillan WO, Jiggins CD. 2021. Rampant Genome-Wide Admixture across the *Heliconius* Radiation Pisani, D, editor. Genome Biology and Evolution. 13. doi: 10.1093/gbe/evab099.

Krueger F. 2015. TrimGalore!: A wrapper around Cutadapt and FastQC to consistently apply adapter and quality trimming to FastQ files, with extra functionality for RRBS data. https://github.com/FelixKrueger/TrimGalore.

Kuhn RM, Haussler D, Kent WJ. 2013. The UCSC genome browser and associated tools. Briefings in Bioinformatics. 14:144–161. doi: 10.1093/bib/bbs038.

Lee H-H, Behringer RR. 2007. Conditional Expression of Wnt4 during Chondrogenesis Leads to Dwarfism in Mice Zwaka, T, editor. PLoS ONE. 2:e450. doi: 10.1371/journal.pone.0000450.

Lewis JJ, Reed RD. 2019. Genome-Wide Regulatory Adaptation Shapes Population-Level Genomic Landscapes in *Heliconius* Wittkopp, P, editor. Molecular Biology and Evolution. 36:159–173. doi: 10.1093/molbev/msy209.

Li J, Wang P, Xie Z, Wang S, Cen S, et al. 2019. TRAF4 positively regulates the osteogenic differentiation of mesenchymal stem cells by acting as an E3 ubiquitin ligase to degrade Smurf2. Cell Death Differ. 26:2652–2666. doi: 10.1038/s41418-019-0328-3.

Liu N, Garry GA, Li S, Bezprozvannaya S, Sanchez-Ortiz E, et al. 2017. A Twist2-dependent progenitor cell contributes to adult skeletal muscle. Nat Cell Biol. 19:202–213. doi: 10.1038/ncb3477.

Losos JB. 1990. Ecomorphology, Performance Capability, and Scaling of West Indian *Anolis* Lizards: An Evolutionary Analysis. Ecological Monographs. 60:369–388. doi: 10.2307/1943062.

Losos JB. 2011. *Lizards in an evolutionary tree: ecology and adaptive radiation of anoles*. University of California Press: Berkeley, Calif.

Losos JB, Andrews RM, Sexton OJ, Schuler AL. 1991. Behavior, Ecology, and Locomotor Performance of the Giant Anole, *Anolis frenatus*. Caribbean Journal of Science. 27:173–179.

Lucek K, Giménez MD, Joron M, Rafajlović M, Searle JB, et al. 2023. The Impact of Chromosomal Rearrangements in Speciation: From Micro- to Macroevolution. Cold Spring Harb Perspect Biol. 15:a041447. doi: 10.1101/cshperspect.a041447.

Mahler DL, Revell LJ, Glor RE, Losos JB. 2010. Ecological Opportunity and the Rate of Morphological Evolution in the Diversification of Greater Antillean Anoles: Opportunity and Rate in *Anolis* Lizards. Evolution. 64:2731–2745. doi: 10.1111/j.1558-5646.2010.01026.x.

Mallo M. 2018. Reassessing the Role of Hox Genes during Vertebrate Development and Evolution. Trends in Genetics. 34:209–217. doi: 10.1016/j.tig.2017.11.007.

Mallo M. 2020. The vertebrate tail: a gene playground for evolution. Cell. Mol. Life Sci. 77:1021–1030. doi: 10.1007/s00018-019-03311-1.

Marques DA, Meier JI, Seehausen O. 2019. A Combinatorial View on Speciation and Adaptive Radiation. Trends in Ecology & Evolution. 34:531–544. doi: 10.1016/j.tree.2019.02.008.

Martin CH, Richards EJ. 2019. The Paradox Behind the Pattern of Rapid Adaptive Radiation: How Can the Speciation Process Sustain Itself Through an Early Burst? Annu. Rev. Ecol. Evol. Syst. 50:569–593. doi: 10.1146/annurev-ecolsys-110617-062443.

Martinez JR, Dhawan A, Farach-Carson MC. 2018. Modular Proteoglycan Perlecan/HSPG2: Mutations, Phenotypes, and Functions. Genes. 9:556. doi: 10.3390/genes9110556.

Massagué J. 2012. TGFβ signalling in context. Nat Rev Mol Cell Biol. 13:616–630. doi: 10.1038/nrm3434.

McGee MD, Borstein SR, Meier JI, Marques DA, Mwaiko S, et al. 2020. The ecological and genomic basis of explosive adaptive radiation. Nature. 586:75–79. doi: 10.1038/s41586-020-2652-7.

Mérot C, Oomen RA, Tigano A, Wellenreuther M. 2020. A Roadmap for Understanding the Evolutionary Significance of Structural Genomic Variation. Trends in Ecology & Evolution. 35:561–572. doi: 10.1016/j.tree.2020.03.002.

Mohammadabadi M, Bordbar F, Jensen J, Du M, Guo W. 2021. Key Genes Regulating Skeletal Muscle Development and Growth in Farm Animals. Animals. 11:835. doi: 10.3390/ani11030835.

Mou Y, Li M, Liu M, Wang J, Zhu G, et al. 2022. OPTN variants in ALS cases: a case report of a novel mutation and literature review. Neurol Sci. 43:5391–5396. doi: 10.1007/s10072-022-06125-5.

Muñoz MM, Frishkoff LO, Pruett J, Mahler DL. 2023. Evolution of a Model System: New Insights from the Study of *Anolis* Lizards. Annu. Rev. Ecol. Evol. Syst. 54:475–503. doi: 10.1146/annurev-ecolsys-110421-103306.

Murrell B, Wertheim JO, Moola S, Weighill T, Scheffler K, et al. 2012. Detecting Individual Sites Subject to Episodic Diversifying Selection Malik, HS, editor. PLoS Genet. 8:e1002764. doi: 10.1371/journal.pgen.1002764.

Naot D, Cornish J. 2008. The role of peptides and receptors of the calcitonin family in the regulation of bone metabolism. Bone. 43:813–818. doi: 10.1016/j.bone.2008.07.003.

Olmo E. 2005. Rate of Chromosome changes and Speciation in Reptiles. Genetica. 125:185–203. doi: 10.1007/s10709-005-8008-2.

Parra-Olea G, Wake DB. 2001. Extreme morphological and ecological homoplasy in tropical salamanders. Proc. Natl. Acad. Sci. U.S.A. 98:7888–7891. doi: 10.1073/pnas.131203598.

Pirani RM, Arias CF, Charles K, Chung AK, Curlis JD, et al. 2023. A high-quality genome for the slender anole (*Anolis apletophallus*): an emerging model for field studies of tropical ecology and evolution Campbell, P, editor. G3: Genes, Genomes, Genetics. 14. doi: 10.1093/g3journal/jkad248.

Poe S, Nieto-montes De Oca A, Torres-carvajal O, De Queiroz K, Velasco JA, et al. 2017. A Phylogenetic, Biogeographic, and Taxonomic study of all Extant Species of *Anolis* (Squamata; Iguanidae). Systematic Biology. 66:663–697. doi: 10.1093/sysbio/syx029.

Pörtner H. 2001. Climate change and temperature-dependent biogeography: oxygen limitation of thermal tolerance in animals. Naturwissenschaften. 88:137–146. doi: 10.1007/s001140100216.

Putnam NH, O'Connell BL, Stites JC, Rice BJ, Blanchette M, et al. 2016. Chromosome-scale shotgun assembly using an in vitro method for long-range linkage. Genome Res. 26:342–350. doi: 10.1101/gr.193474.115.

QGIS.org. 2020. QGIS Geographic Information System. http://www.qgis.org.

R Core Team. 2022. R: A language and environment for statistical computing. https://www.R-project.org/.

Ríos-Orjuela JC, Camacho-Bastidas JS, Jerez A. 2020. Appendicular morphology and locomotor performance of two morphotypes of continental anoles: *Anolis heterodermus* and *Anolis tolimensis*. Journal of Anatomy. 236:252–273. doi: 10.1111/joa.13092.

Ritzman TB, Stroik LK, Julik E, Hutchins ED, Lasku E, et al. 2012. The Gross Anatomy of the Original and Regenerated Tail in the Green Anole (*Anolis carolinensis*). The Anatomical Record. 295:1596–1608. doi: 10.1002/ar.22524.

Rodríguez A, Rusciano T, Hamilton R, Holmes L, Jordan D, et al. 2017. Genomic and phenotypic signatures of climate adaptation in an *Anolis* lizard. Ecology and Evolution. 7:6390–6403. doi: 10.1002/ece3.2985.

Rossi M, Buonuomo PS, Battafarano G, Conforti A, Mariani E, et al. 2020. Dissecting the mechanisms of bone loss in Gorham-Stout disease. Bone. 130:115068. doi: 10.1016/j.bone.2019.115068.

Rotwein P. 2018. Insulinlike Growth Factor 1 Gene Variation in Vertebrates. Endocrinology. 159:2288–2305. doi: 10.1210/en.2018-00259.

Rovatsos M, Altmanová M, Pokorná M, Kratochvíl L. 2014. Conserved Sex Chromosomes Across Adaptively Radiated *Anolis* Lizards: Brief Communication. Evolution. 68:2079–2085. doi: 10.1111/evo.12357.

Rubin C-J, Enbody ED, Dobreva MP, Abzhanov A, Davis BW, et al. 2022. Rapid adaptive radiation of Darwin's finches depends on ancestral genetic modules. Sci. Adv. 8. doi: 10.1126/sciadv.abm5982.

Sakamoto F, Kanamori S, Díaz LM, Cádiz A, Ishii Y, et al. 2024. Detection of evolutionary conserved and accelerated genomic regions related to adaptation to thermal niches in *Anolis* lizards. Ecology and Evolution. 14:e11117. doi: 10.1002/ece3.11117.

Schluter D. 2000. *The Ecology of adaptative radiation*. Oxford University press: Oxford.

Schneider CA, Rasband WS, Eliceiri KW. 2012. NIH Image to ImageJ: 25 years of image analysis. Nat Methods. 9:671–675. doi: 10.1038/nmeth.2089.

Schrader L, Schmitz J. 2019. The impact of transposable elements in adaptive evolution. Molecular Ecology. 28:1537–1549. doi: 10.1111/mec.14794.

Seebacher F, Murray SA, Else PL. 2009. Thermal Acclimation and Regulation of Metabolism in a Reptile (*Crocodylus porosus*): The Importance of Transcriptional Mechanisms and Membrane Composition. Physiological and Biochemical Zoology. 82:766–775. doi: 10.1086/605955.

Seehausen O, Butlin RK, Keller I, Wagner CE, Boughman JW, et al. 2014. Genomics and the origin of species. Nat Rev Genet. 15:176–192. doi: 10.1038/nrg3644.

Seixas FA, Edelman NB, Mallet J. 2021. Synteny-Based Genome Assembly for 16 Species of*Heliconius*Butterflies, and an Assessment of Structural Variation across the Genus Gonzalez, J, editor. Genome Biology and Evolution. 13. doi: 10.1093/gbe/evab069.

Shiels H, Li X, Schumacker PT, Maltepe E, Padrid PA, et al. 2000. TRAF4 Deficiency Leads to Tracheal Malformation with Resulting Alterations in Air Flow to the Lungs. The American Journal of Pathology. 157:679–688. doi: 10.1016/s0002-9440(10)64578-6.

Shindo T, Tanaka M, Kamiyoshi A, Ichikawa-Shindo Y, Kawate H, et al. 2019. Regulation of cardiovascular development and homeostasis by the adrenomedullin-RAMP system. Peptides. 111:55–61. doi: 10.1016/j.peptides.2018.04.004.

Shiraishi S, Nakamura Y-N, Iwamoto H, Haruno A, Sato Y, et al. 2006. S-myotrophin promotes the hypertrophy of skeletal muscle of mice in vivo. The International Journal of Biochemistry & Cell Biology. 38:1114–1122. doi: 10.1016/j.biocel.2005.11.014.

Shu B, Zhang M, Xie R, Wang M, Jin H, et al. 2011. BMP2, but not BMP4, is crucial for chondrocyte proliferation and maturation during endochondral bone development. Journal of Cell Science. 124:3428–3440. doi: 10.1242/jcs.083659.

Silva FA, Souza ÉMS, Ramos E, Freitas L, Nery MF. 2023. The molecular evolution of genes previously associated with large sizes reveals possible pathways to cetacean gigantism. Sci Rep. 13. doi: 10.1038/s41598-022-24529-3.

Simão FA, Waterhouse RM, Ioannidis P, Kriventseva EV, Zdobnov EM. 2015. BUSCO: assessing genome assembly and annotation completeness with single-copy orthologs. Bioinformatics. 31:3210–3212. doi: 10.1093/bioinformatics/btv351.

Smit AFA, Hubley R, Green P. 2015. RepeatMasker.

Soccio RE, Adams RM, Romanowski MJ, Sehayek E, Burley SK, et al. 2002. The cholesterol-regulated StarD4 gene encodes a StAR-related lipid transfer protein with two closely related homologues, StarD5 and StarD6. Proc. Natl. Acad. Sci. U.S.A. 99:6943–6948. doi: 10.1073/pnas.052143799.

Stanke M, Keller O, Gunduz I, Hayes A, Waack S, et al. 2006. AUGUSTUS: ab initio prediction of alternative transcripts. Nucleic Acids Research. 34:W435–W439. doi: 10.1093/nar/gkl200.

Stroud JT, Losos JB. 2016. Ecological Opportunity and Adaptive Radiation. Annu. Rev. Ecol. Evol. Syst. 47:507–532. doi: 10.1146/annurev-ecolsys-121415-032254.

Sun B, Williams CM, Li T, Speakman JR, Jin Z, et al. 2022. Higher metabolic plasticity in temperate compared to tropical lizards suggests increased resilience to climate change. Ecological Monographs. 92:e1512. doi: 10.1002/ecm.1512.

Supek F, Bošnjak M, Škunca N, Šmuc T. 2011. REVIGO Summarizes and Visualizes Long Lists of Gene Ontology Terms Gibas, C, editor. PLoS ONE. 6:e21800. doi: 10.1371/journal.pone.0021800.

Szklarczyk D, Gable AL, Lyon D, Junge A, Wyder S, et al. 2019. STRING v11: protein–protein association networks with increased coverage, supporting functional discovery in genome-wide experimental datasets. Nucleic Acids Research. 47:D607–D613. doi: 10.1093/nar/gky1131.

Tejedor G, Laplace-Builhé B, Luz-Crawford P, Assou S, Barthelaix A, et al. 2020. Whole embryo culture, transcriptomics and RNA interference identify TBX1 and FGF11 as novel regulators of limb development in the mouse. Sci Rep. 10. doi: 10.1038/s41598-020-60217-w.

the Genetic Factors for Osteoporosis (GEFOS) Consortium. 2009. Twenty bone-mineral-density loci identified by large-scale meta-analysis of genome-wide association studies. Nat Genet. 41:1199–1206. doi: 10.1038/ng.446.

Tollis M, Hutchins ED, Stapley J, Rupp SM, Eckalbar WL, et al. 2018. Comparative Genomics Reveals Accelerated Evolution in Conserved Pathways during the Diversification of Anole Lizards. Genome Biology and Evolution. 10:489–506. doi: 10.1093/gbe/evy013.

Velasco JA, Martínez-Meyer E, Flores-Villela O, García A, Algar AC, et al. 2016. Climatic niche attributes and diversification in *Anolis* lizards. Journal of Biogeography. 43:134–144. doi: 10.1111/jbi.12627.

Vouyovitch CM, Perry JK, Liu DX, Bezin L, Vilain E, et al. 2016. WNT4 mediates the autocrine effects of growth hormone in mammary carcinoma cells. Endocrine-Related Cancer. 23:571–585. doi: 10.1530/erc-15-0528.

Wagner G, Fenzl A, Lindroos-Christensen J, Einwallner E, Husa J, et al. 2021. LMO3 reprograms visceral adipocyte metabolism during obesity. J Mol Med. 99:1151–1171. doi: 10.1007/s00109-021-02089-9.

Wang RN, Green J, Wang Z, Deng Y, Qiao M, et al. 2014. Bone Morphogenetic Protein (BMP) signaling in development and human diseases. Genes & Diseases. 1:87–105. doi: 10.1016/j.gendis.2014.07.005.

Wang Y, Li J, Yao X, Li W, Du H, et al. 2017. Loss of CIB2 Causes Profound Hearing Loss and Abolishes Mechanoelectrical Transduction in Mice. Front. Mol. Neurosci. 10. doi: 10.3389/fnmol.2017.00401.

Ward AB, Mehta RS. 2010. Axial Elongation in Fishes: Using Morphological Approaches to Elucidate Developmental Mechanisms in Studying Body Shape. Integrative and Comparative Biology. 50:1106–1119. doi: 10.1093/icb/icq029.

Wellborn GA, Langerhans RB. 2015. Ecological opportunity and the adaptive diversification of lineages. Ecology and Evolution. 5:176–195. doi: 10.1002/ece3.1347.

Wogan GOU, Yuan ML, Mahler DL, Wang IJ. 2023. Hybridization and Transgressive Evolution Generate Diversity in an Adaptive Radiation of *Anolis* Lizards Burbrink, F, editor. Systematic Biology. 72:874–884. doi: 10.1093/sysbio/syad026.

Wollenberg Valero KC, Pathak R, Prajapati I, Bankston S, Thompson A, et al. 2014. A candidate multimodal functional genetic network for thermal adaptation. PeerJ. 2:e578. doi: 10.7717/peerj.578.

Ye Z, Kimelman D. 2020. *hox13* genes are required for mesoderm formation and axis elongation during early zebrafish development. Development. doi: 10.1242/dev.185298.

Zecchini S, Giovarelli M, Perrotta C, Morisi F, Touvier T, et al. 2019. Autophagy controls neonatal myogenesis by regulating the GH-IGF1 system through a NFE2L2- and DDIT3-mediated mechanism. Autophagy. 15:58–77. doi: 10.1080/15548627.2018.1507439.

Zhang Quanlong, Pan Y, Ji J, Xu Y, Zhang Qiaoyan, et al. 2021. Roles and action mechanisms of WNT4 in cell differentiation and human diseases: a review. Cell Death Discov. 7. doi: 10.1038/s41420-021-00668-w.

Zhang Yu, Yang X, Zhu X-L, Bai H, Wang Z-Z, et al. 2021. S100A gene family: immune-related prognostic biomarkers and therapeutic targets for low-grade glioma. Aging. 13:15459–15478. doi: 10.18632/aging.203103.

Zheng Q-W, Ni Q-Z, Zhu B, Liang X, Ma N, et al. 2022. PPDPF promotes lung adenocarcinoma progression via inhibiting apoptosis and NK cell-mediated cytotoxicity through STAT3. Oncogene. 41:4244–4256. doi: 10.1038/s41388-022-02418-3.

Zhu J, Xu M, Liu Y, Zhuang L, Ying K, et al. 2019. Phosphorylation of PLIN3 by AMPK promotes dispersion of lipid droplets during starvation. Protein Cell. 10:382–387. doi: 10.1007/s13238-018-0593-9.

Zhu S, Chim SM, Cheng T, Ang E, Ng B, et al. 2016. Calmodulin interacts with Rab3D and modulates osteoclastic bone resorption. Sci Rep. 6. doi: 10.1038/srep37963.